➤ 6.3. USAXS – Ultra-small-angle X-ray scattering for materials science

by Jan Ilvasky, X-Ray Science Division, Advanced Photon Source, Argonne National Laboratory, and Fan Zhang, Material Measurement Laboratory, National Institute of Standards and Technology

6.3.1 Introduction

Ultra-small-angle scattering refers to small-angle scattering collected for scattering vectors q smaller than 0.001 $Å^{-1}$ of X-rays (USAXS) or neutrons (USANS). Using $d = \pi / q_{min}$, where q_{min} is the minimal q that the instrument can access, the typical maximum dimensions (d_{max}) characterized by USAXS/USANS are greater than 300 nm. Currently, the state-of-the-art USAXS instruments routinely achieve a q_{min} of ≈ 10^{-4} Å-1 or a d_{max} of ≈ 3 μm, and USANS instruments can achieve a q_{min} of ≈ 10-5 Å or a d_{max} of ≈ 30 μm. These dimensions often provide unique insight into features that would typically require imaging techniques. Scattering offers capabilities that may be difficult to obtain from, and are complementary to, imaging – scattering results are statistically representative because of the larger sample volume. When placed on absolute intensity scales, scattering techniques provide information regarding the scattering objects' size, shape, specific surface area, and absolute volume. The scattering methods are also nondestructive and can accommodate complex sample environments, enabling in-situ or ex-situ experiments for samples that are not optically transparent or lack optical contrast. Such advantages make USAXS/SAXS techniques uniquely useful for studies of complex materials with hierarchical structures such as polymers, metals and alloys, natural materials (such as minerals, sediments, and soils), and many more.

For the USAXS instrument, q_{min} defines the smallest accessible q. An often-overlooked component is that USAXS instruments must have a meaningful q resolution, q_{res}, especially for the data points close to $q$min, because a significant number of data points in the ultra-small-angle range are required to describe and interpret the

structures of interest. For the USAXS instrument in a Bonse-Hart geometry (see below), the q_{res} is defined by the width of the crystal rocking curve and is similar to q_{min}, allowing for 10 or more meaningful data points below 0.001 $Å^{-1}$. For pinhole-based USAXS instruments, one must be conscientious about this criterion and carefully evaluate the q_{res} based on the targeted X-ray energy, the detector pixel size, and other geometrical parameters.

As alluded to above, the two types of standard USAXS instruments are 1) long pinhole cameras (e.g., ID02 at ESRF and P03 at PETRA III) with a focused X-ray beam and 2) Bonse-Hart-type devices available as desktop instruments and a synchrotron instrument (APS USAXS). Between these two types of designs, the Bonse-Hart devices are more compact and can measure sizes up to four decades in q. Furthermore, when combined with a supplementary high-performance SAXS camera and an X-ray diffraction camera (XRD, or wide-angle X-ray scattering, WAXS), a superior measurement capability is created which covers five or more decades in q and enables comprehensive structural characterizations from less than an angstrom to several micrometers. These attributes make the Bonse-Hart devices the most popular choice to access the USAXS regime in commercial desktop setups. We emphasize that Bonse-Hart and pinhole USAXS devices have their respective advantages and disadvantages, making these two configurations more complementary than competitive. Proper selection of the most appropriate configuration is essential for successful experiments, and so is the proper selection of other experimental conditions, such as type of radiation (X-rays or neutrons), X-ray wavelength, and sample environment.

The Bonse–Hart geometry, which utilizes crystal optics, has a high angular resolution defined by the width of the crystal rocking curve. It is worth mentioning that the Bonse-Hart geometry finds applications in both X-ray and neutron scattering. While USAXS and USANS share the same general principles, they have their niches and advantages. For example, the crystal rocking curve of neutrons is significantly narrower than its X-ray counterpart, allowing

USANS instruments to access a size ≈ 10 × d_{max} for USAXS with the same crystals. The Bonse-Hart USANS instruments are available as dedicated user instruments at several neutron-scattering facilities worldwide (ILL, NIST, ORNL, and ANSTO). However, they fall outside the scope of this chapter.

For the rest of this chapter, we will further discuss the Bonse-Hart-type USAXS instruments, which have been used for ultra-small-angle scattering experiments for more than 40 years.[148]-[151] We will focus on USAXS and provide an overview of its development state and technical capability in the form of desktop instruments or dedicated synchrotron facilities. We will use USAXS and Bonse-Hart USAXS interchangeably, unless specified otherwise.

6.3.2 Bonse-Hart instrumentation

The Bonse-Hart device (Fig. 51) utilizes two pairs of crystals. Here, we assume the crystals reflect the X-ray beam vertically, but horizontally scattering devices are also available.[152] In a USAXS measurement, a monochromatic X-ray beam first arrives at a pair of channel-cut crystals, referred to as collimating crystals, that collimates the X-ray beam. The crystal optics have an angular acceptance window of approximately the full width at half maximum (FWHM) of the double-crystal rocking curve. This acceptance window is extremely narrow, allowing only the X-ray beam parallel within the acceptance angle to pass through. For example, at 21 keV, Si (111) optics has an FWHM of ≈ 17.2 μrad (3.5 arcsec), ensuring the exiting beam is highly parallel along the vertical direction. Once aligned, the collimating crystals remain stationary. After the collimated beam encounters the sample, small-angle scattering events occur. A rotating second set of crystal optics, placed after the sample, resolves the scattered beam. This second pair of crystals, known as analyzer crystals, probes the angular intensity distribution of the scattered beam and provides the point-wise data acquisition for the USAXS data. We also note that in the schematics below, the collimation only occurs along the vertical direction,

and the beam divergence along the horizontal direction is significantly larger. This disparity in orientationally dependent collimating conditions creates a slit-smearing geometry, requiring post-experiment data analysis to acquire the proper differential scattering cross-section.

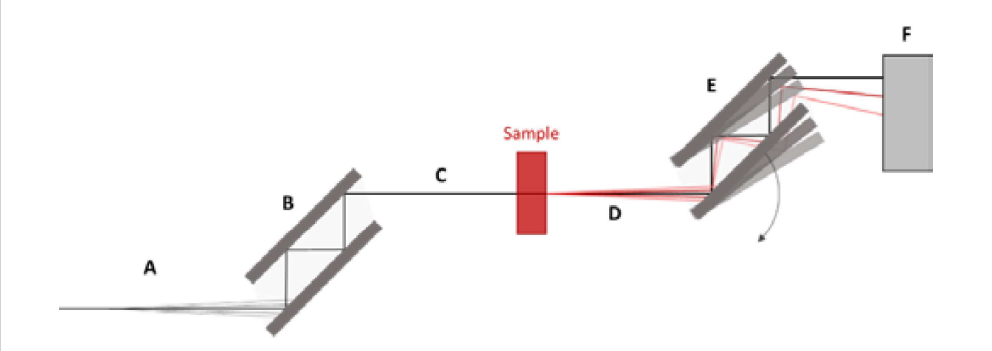

Fig. 51
Schematics of Bonse-Hart device: Uncollimated primary beam (A), collimating channel-cut crystals (B), vertically collimated (parallel) primary beam after the collimator (C), primary beam which has passed through the sample, includes attenuated primary beam with addition of sample scattering (D), rotating analyzer channel-cut crystal (E), X-ray detector (F).

Bonse-Hart USAXS data acquisition requires two measurements. First, without the sample, one acquires the instrumental profile ("empty" or "blank"), including the crystal rocking curve and other instrumental scattering signatures such as air scattering, scattering from crystal surfaces, slits, and any X-ray windows. The second measurement requires the sample in the beam, and the acquired scattering curve combines both the instrumental profile and the sample scattering profile. The difference between these two rocking curve profiles (after normalization and transmission correction) is the (slit-smeared, see below) scattering of the sample.

Because USAXS data acquisition involves rotation of the analyzer crystals, USAXS instruments are much slower than the pinhole SAXS instruments, where all q values are collected at once. Hence, when measurement efficiency is essential, in, e.g., in-situ experiments, we must consider the data collection strategy for USAXS measurements to enable an efficient throughput. Two common measurement strategies exist for USAXS measurements: step

scan or fly scan. In step scan mode, the analyzer crystals move over a pre-determined set of angles (q) and collect data for a pre-defined time at each angle. In the fly-scan mode, the analyzer crystals rotate continuously with simultaneous data acquisition. The fly-scan mode does not involve repeated starts, stops, and counting cycles. Hence, the measurement is typically faster and more X-ray efficient. However, during a fly scan, the measured intensity at each resulting q represents integrated intensities acquired over a range of angles (qs), resulting in additional smearing that modifies the instrumental q-resolution. The step-scan mode does not have this movement-induced smearing issue. Furthermore, one must recognize that it is impractical to use linearly spaced steps because of the wide range of q the USAXS instruments cover. A common practice is to define an array of measurement angles (q) on a semi-logarithmic scale, with small steps at the smallest measurement angles and progressively increasing step sizes towards higher angles. A rule of thumb is to have 10 to 50 points per decade in q, a data density suitable for most USAXS applications. Because of these limitations, the Bonse-Hart USAXS data collection will always be slower than the pinhole SAXS, and USAXS data points will have worse counting statistics.

Bonse-Hart USAXS instruments can measure scattering data over a broad q-range. For example, the APS USAXS instrument has provided measurement capability from 10^{-4} Å^{-1} to ≈ 1 Å^{-1} since the early 2000s. However, because the SAXS intensity typically decreases asymptotically following q^{-4} (in the slit-smeared case, q^{-3}), the instrumental q-range also depends on the X-ray flux on the sample and detector capabilities. Desktop instruments with a typical flux ≈ 10^7 photon/s can realistically measure about two decades in q (typically from 0.0002 Å^{-1} to 0.01 Å^{-1}) with a data collection time between 10 min and 30 min, depending on the sample's scattering power. Synchrotron instruments, with an undulator or bending-magnet source, may have X-ray flux exceeding 10^{12} photon/s, enabling access to a q value of 0.3 Å^{-1} or higher with a data collection time of minutes.[153]-[155] However, the counting statistics above q=0.1 Å^{-1} are poor even with synchrotron measurements.

A unique feature of the Bonse-Hart geometry is that the beam size has no impact on the *q*-resolution of the instrument because the *q*-resolution is related only to crystal optics and potentially data collection strategy (e.g., fly scanning as described above). The USAXS instruments routinely utilize beam sizes ≈ 1 mm^2 and USANS instruments even 1 cm^2. This feature is valuable because the illuminated sample volume can be substantial, yielding excellent sampling statistics. For example, the APS USAXS instrument, when operated at 21 keV, enables the measurements of water-based samples that are 4 mm thick. With a beam size of 1 mm x 1 mm, the sample volume is 4 mm^3. This large, illuminated sample volume enabled by USAXS may be necessary when the scattering objects have low concentrations or contain significant inhomogeneities, thus circumventing the sampling challenges experienced by typical pinhole SAXS instruments, especially those utilizing a focused beam.

Bonse-Hart devices also have different requirements for their detectors compared to typical pinhole SAXS instruments. While USAXS detectors do not require spatial resolution because of their point-wise detection, they need to have a sizeable linear-intensity dynamic range, high efficiency, and low noise. The extensive linear-intensity dynamic range is critical and requires further explanation. For USAXS measurements, the detector needs to take on the whole, direct beam, where the beam can have a photon density exceeding 10^{12} photon/s at a synchrotron source. Meanwhile, the detector must have linearity and sensitivity to measure the scattering intensity near the background level, which is often six to ten decades below the direct beam intensity. On the one hand, current desktop Bonse-Hart devices typically reuse their SAXS area detectors with single-photon counting capabilities, such as a PILATUS* or an EIGER* detector. On the other hand, synchrotron-based

* Certain commercial products or company names are identified here to describe our study adequately. Such identification is not intended to imply recommendation or endorsement by the National Institute of Standards and Technology, nor is it intended to imply that the products or names identified are necessarily the best available for the purpose.

USAXS devices use photodiodes combined with high-dynamic-range amplifiers[156] or scintillators equipped with calibrated absorptions filters.[151]

We also note that scattering-based imaging using a Bonse-Hart geometry has been exploited. An imaging detector replaces a photodiode detector to image the transmitted and *q*-specific scattered beam directly. While out of the scope of the current chapter, such imaging methodologies provide visible insight into the degree of the sample inhomogeneities at different length scales.[157][158]

As mentioned previously, the crystal optics defines the excellent q_{min} and *q*-resolution of the Bonse-Hart USAXS instrument. Desktop instruments commonly use Si (111) crystals because these crystals allow the maximum throughput of the direct beam after the collimating crystals. Their q_{min} is $\approx 1.2 \times 10^{-4}$ Å^{-1} with Cu Kα radiation. Other options with higher-order crystal optics exist, allowing an even smaller q_{min}, as demonstrated in Fig. 52. For example, Si (220) and Si (440) crystal optics theoretically enable a qmin of $\approx 0.8 \times 10^{-4}$ Å^{-1} and $\approx 0.3 \times 10^{-4}$ Å^{-1}. The lower FWHM, which gives rise to this better qmin, limits the beam throughput, making these higher-order crystal optics primarily suitable for synchrotron instruments. Even for the synchrotron instruments, this reduction of beam throughput caused by higher-order crystal optics can limit the effective *q*-range of the instrument at the high-*q* end of the scattering profile because the photodiode captures fewer scattered photons during a specific measurement duration.

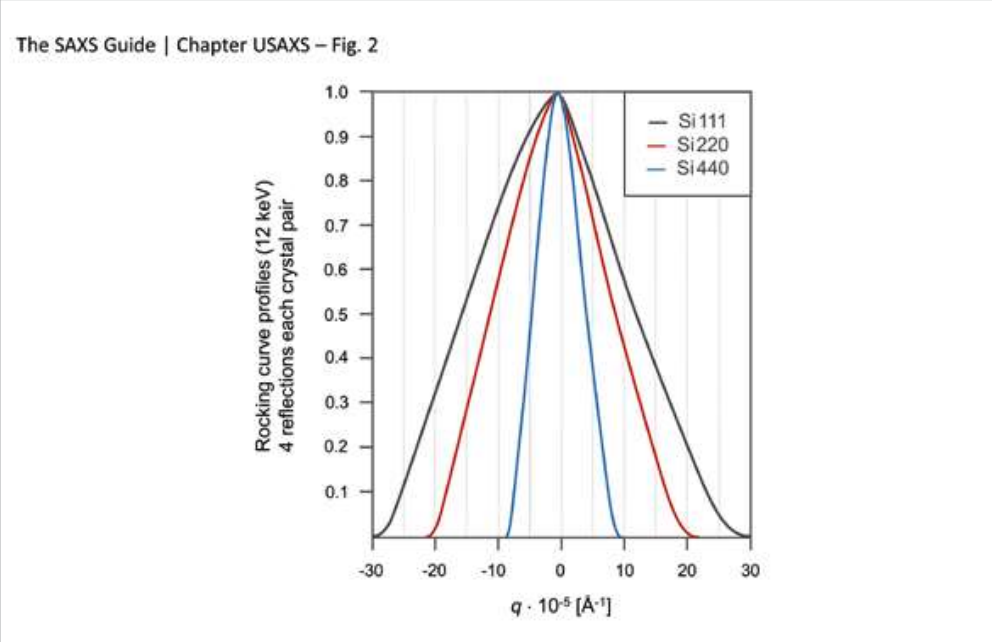

Fig. 52
Comparison for rocking curve widths for Si 111, 220, 440 at 12 keV for four reflections. The higher order planes lead to a narrower rocking curve and enable a smaller accessible qmin and a higher q resolution.

The performance of Bonse-Hart devices also depends on the number of Bragg reflections in each pair of crystals. While the number of reflections does not change the FWHM of the double-crystal curve, it changes the rocking curve profile shape. An increase in the number of reflections reduces the intensity at the tail of the rocking curve and improves the instrument's sensitivity by suppressing its natural background.[159] We believe the minimum number of reflections for USAXS is three in each crystal pair, a criterion also commonly used in the USANS instrument. An odd number of reflections in each crystal pair causes the beam to change direction significantly, which can be advantageous when suppressing background in the detector is critical, such as in the case of USANS. For X-rays, this creates a challenge because the new beam direction is energy-dependent since it follows the Bragg condition. This energy dependency makes it complicated for a USAXS instrument with changeable energy and is usually only adopted for fixed-energy instruments. Most USAXS instruments today utilize four (or six) reflections in each crystal pair. In this case, the beam retains its original direction, hence making changes in X-ray energy much easier to accommodate. Fig. 51 illustrates a case of four reflections in two parallel crystals in both the analyzer and the collimating crystal pairs. For each pair, the outgoing beam is vertically offset

by a small distance determined by the number of reflections, the gap between the crystals, and the scattering angle while maintaining the same direction as the incident beam. Some desktop instruments utilize Bartell channel cut crystals, where the beam direction after four reflections is the same as the incoming beam direction. However, this setup is less X-ray efficient due to Bartell crystal's lower throughput.[160]

The concept of slit smearing, while not unique to Bonse-Hart devices, is critical for data analysis. The detected scattering intensity at a given q in a slit-smeared Bonse-Hart USAXS instrument contains scattering data over a solid angle shaped like a rectangle. In angular terms, the rectangle's minor dimension is defined by the FWHM of the crystal optics. Its major dimension is primarily related to the size and shape of the detector and the sample-to-detector distance. When expressed in a q unit, this major dimension is known as the slit length. When the slit length is less than qmax, we consider the slit length finite. Here, q_{max} is the maximum q of a USAXS measurement. When it is comparable to or greater than q_{max}, we consider the slit length infinite. The distinction between finite slit length and infinite slit length is essential because it impacts data processing and the USAXS instrument's ability to place data on an absolute intensity scale. While devices with finite slit length can place data on an absolute intensity scale using first principles by calculating the solid angle, acquiring absolute intensity data is much more difficult (if not impossible) for devices with infinite slit length.

In mathematical terms, the measured intensity follows

Equation 62

$$I(q) = \Phi_0 \, A \, t \, T \, \epsilon \, \Omega \frac{d\Sigma(q)}{d\Omega}$$

Here, A is the illumination area, t is sample thickness, T is sample transmission, $\Phi 0$ is the incident flux in the unit of photon/s/area, ϵ is the detector efficiency, and $d\sum(q)/d\Omega$ represents the differential scattering cross-section per unit volume per unit angle. In a

slit-smeared USAXS measurement, the observational solid angle is the size of the slit, defined as slit height along the q direction (typically, the rocking curve FWHM described above) × the slit length. If the slit length is infinite, numerically, the solid angle loses meaning and becomes effectively unknown. However, in everyday practice, we can assume a maximum slit length of 4p/*l*, which is significantly larger than q_{max}, to circumvent this restriction and allow absolute calibration.

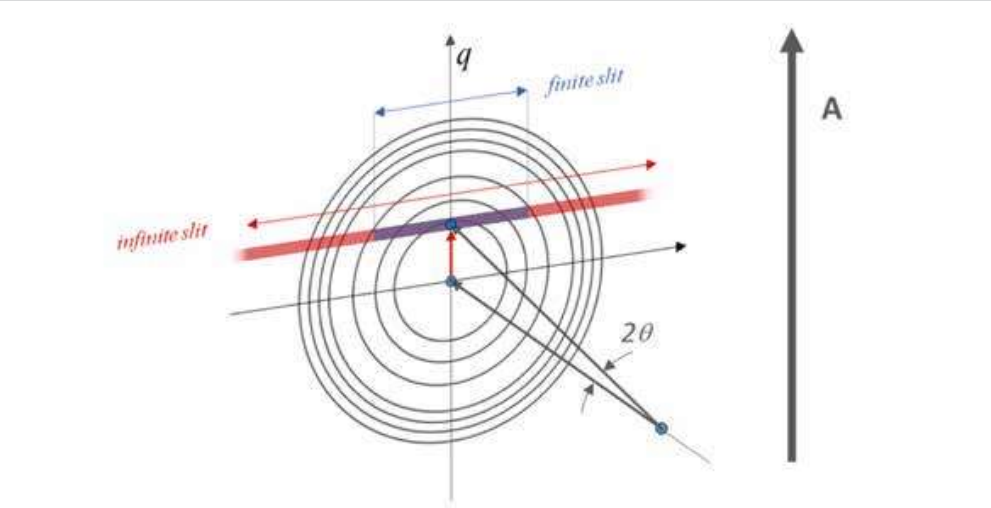

Fig. 53
Schematics of finite slit scanning: the red area represents the infinite slit and the blue area the finite slit (for the finite slit, the slit length is half of the slit dimension shown in the figure). A represents the scanning direction, 2θ is the scattering angle, and ***q*** *is the scattering vector.*

Slit smearing impacts the applicability of Bonse-Hart USAXS instruments, especially for materials with anisotropic scattering profiles, because slit smearing integrates the scattering signal within the observing solid-angle non-discriminatorily. Based on the experimental slit-smeared data, it is possible to reconstruct a pinhole-collimated scattering profile using various desmearing routines, such as the Lake Method.[20] We strongly recommend smearing the model using a slit calculated from the known instrumental parameters and performing least-squares or other optimization routines using the smeared model on the smeared data. Nevertheless, in either case, the basic assumption is that the scattering data is isotropic. When this assumption does not hold, the data-desmearing or model-smearing approach breaks down, and rigorous and quantitative data analysis becomes difficult or impossible. For this reason, we strongly advocate using a long-pinhole USAXS instrument for materials with known microstructural anisotropy.

Finally, we note that 2D-collimated Bonse-Hart devices have been developed to measure anisotropically scattering samples. These devices use two collimating crystal pairs (one vertical and one horizontal) and two analyzer crystal pairs (one vertical and one horizontal). These crystals define a slight solid angle; the devices become SAXS instruments with an ultra-high resolution. The usage of four pairs of crystal optics also makes the instrument much less X-ray-efficient. Therefore, it is only usable at synchrotrons with highly collimated X-ray sources and high photon flux.[151] Data acquired by such devices no longer require a desmearing routine, and it is possible to rotate the analyzer crystals to map the reciprocal space, albeit with low efficiency. The 2D collimation also places a stringent requirement on the absolute intensity measurements – the crystal tilts in both crystal planes must be centered to ensure that the $q = 0$ position in the scanning direction is also at zero q in the orthogonal plane. Because of these challenges, these 2D-collimated Bonse-Hart devices are rarely used, and long pinhole USAXS instruments are the preferred method to fulfill the measurement need for anisotropic USAXS measurements.

6.3.3 Hierarchical structure in soft materials

Structure hierarchy is the rule, instead of an exception, of nature.[161] From the beauty of DNA, where alternating sugar and phosphate groups self-assemble into a twisted ladder as a double helix, to the superb combination of bending and compressive strength of bone,[162] owing to its uniquely hierarchical structure spanning from sub-nanostructure to macrostructure, nature realizes extraordinary materials properties through the hierarchical organization of molecules to microscopic and macroscopic scales. The pursuit of advanced functional materials with hierarchical structures represents a frontier of not only modern materials science[163] but also human discovery.[164] One central challenge to recapitulate a level of control to precisely create such materials resides in the mastery of control at each structural level, which requires a deterministic characterization of hierarchical materials.

Soft materials, such as polymers and colloids, often form a hierarchical structure. Delineating these structures is essential to developing the application-critical structure-property-performance relationship and requires experimental techniques that resolve microstructures over a large and continuous size range. Moreover, in situ or operando characterization with a time resolution relevant to the transformation of these materials upon external stimuli, such as pressure, temperature, and electrical field, is beneficial. USAXS, especially synchrotron-based USAXS, is well-suited for these applications and provides a unique opportunity to peer into these widely used materials.

In this section, we will present two selected examples to illustrate the exciting science enabled by USAXS and bring forward the vast possibilities for which USAXS may be a suitable characterization tool to contribute to the continued development of materials science benefitting mankind's quality of life.

6.3.3.1 Polymer composite with nanometer-sized reinforcement fillers

Polymer composites with nanometer-sized reinforcement fillers have captured significant imagination from the materials research community because of their potential to drastically improve the materials' mechanical performance at filler loadings at less than 1 % mass. One premier example is the targeted application of nano-silica to replace carbon black as the filler material for automobile tires. This replacement promises to improve the tires' tread life and offers the possibility to enhance the tires' wet-grip properties while providing a more negligible rolling resistance, thereby improving the vehicle's fuel efficiency and reducing its carbon footprint. However, the enhancements to the modulus of the composites with the addition of hard fillers remain marginal, and practical solutions to this problem remain elusive.

Schaefer and Justice, in a now landmark paper, rigorously investigated the filler morphology and critically evaluated the morphology's role in possible modulus enhancement.[165] Using

Dimosil-precipitated silica, a type of precipitate silica with a high specific surface area (100 m^2/g – 400 m^2/g) as an example, they performed structural analysis using the transmission electron microscope, USAXS, and light scattering. The TEM data, shown in Fig. 55(b), clearly demonstrated that the primary particles of the precipitated silica are quasi-spherical and ≈ 20 nm in size with a smooth surface and form aggregates. It is, however, difficult to quantify the size or structure of the aggregates based on TEM data alone.

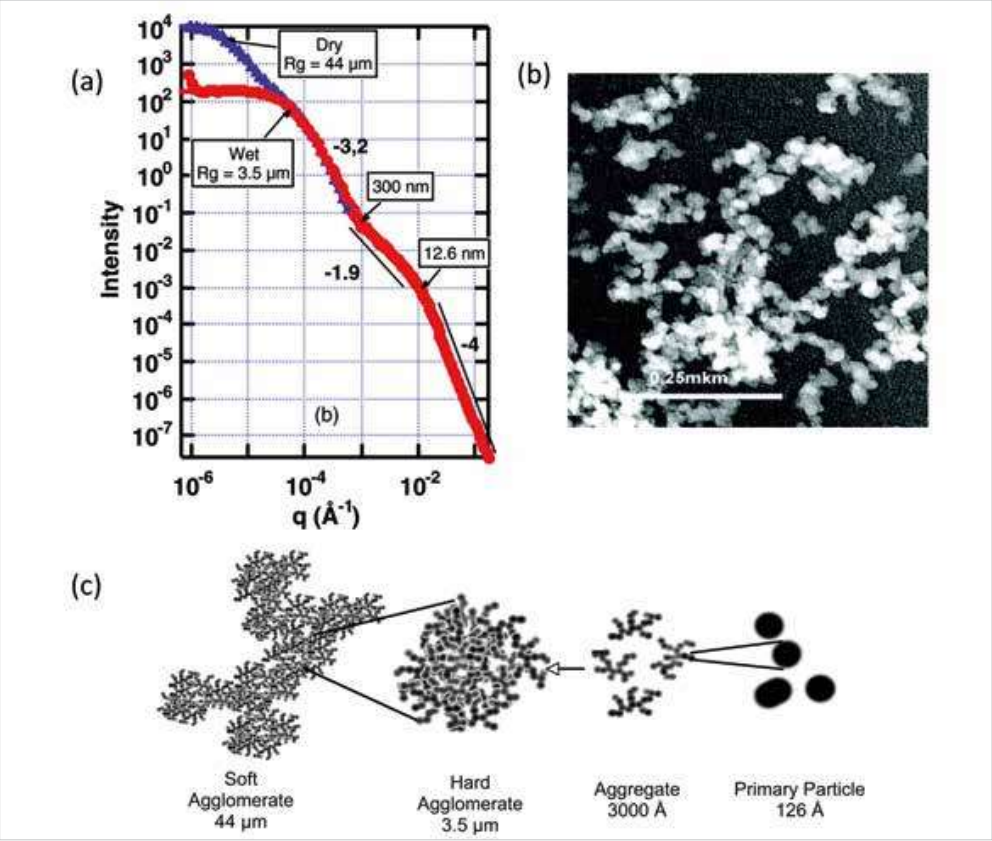

Fig. 54
(a) Combined light scattering and USAXS data revealing different structural levels in the Dimosil-precipitated silica. (b) TEM data showing the primary precipitated silica particles and their aggregates. (c) An illustration of the different structural levels in the precipitated silica. Adapted with permission from [165] Copyright (2007) American Chemical Society .

The scattering data, shown in Fig. 54(a), includes both USAXS and light-scattering data and encompasses a q-range from to ≈ 2×10^{-6} $Å^{-1}$ to 0.3 $Å^{-1}$, and provides conclusive evidence of the existence of structural levels of the Dimosil-precipitated silica in their wet (red) and dry (blue) states. Both the dry and wet silica contain:

- Primary particles ($R_G \approx 13$ nm)
- Aggregates ($R_G \approx 300$ nm)
- Hard agglomerates ($R_G \approx 3.5$ μm)

Here, R_G is the radius of gyration.

The dried product also includes a ≈ 44 μm soft agglomerate whose presence is susceptible to ultrasonic perturbation. This rich structural insight, only available through a scattering experiment with a broad and continuous q-range, unveils the mechanistic basis for the lack of improvement to the modulus of the nanocomposites with the addition of hard fillers. The modulus of a fractal aggregate inversely depends on the aggregate size. The filler nanoparticles in polymer nanocomposites aggregate ubiquitously. Hence, once the aggregate size is adequately significant so that the aggregate modulus is below the matrix modulus, the desired reinforcement effect will not occur. This critical insight points to the importance of filler-morphology control in the commercial success of these nanocomposites, a continued direction in optimizing nanocomposite materials.

6.3.3.2 Structure of binary colloidal suspensions

Colloidal suspensions, also known as colloidal dispersions, involve particles in the size range of a few nanometers to a micrometer dispersed in a fluid medium. Colloidal suspensions are omnipresent in everyday life: they are present, e.g., in ink, paint, blood, and milk.[166] They also form the basis for some of the most advanced functional materials, including colloidal hybrid nanostructures with multiple functionalities,[167] colloidal lipid nanoparticles as drug carriers,[168] and self-assembled colloidal gels with dynamic color tunability.[169] Many of the fundamentals of the colloidal suspensions, such as their thermodynamics, microstructures, and transport properties, can be traced to the delicate interparticle interactions. The variety of the interactions, including electrostatic, steric, and depletion interactions, adds to the richness of colloidal science and provides avenues to tailor the structure and property control

at microscopic and macroscopic levels. Traditionally, static and dynamic light scattering played a significant role in understanding the nature of the colloidal interactions. However, they are of limited use when dealing with concentrated or turbid suspensions. USAXS, in contrast, is less sensitive to multiple scattering common to visible light in concentrated suspensions and provides the appropriate size range to understand the structure of the colloidal suspension, including the form factor, structure factor, and the equation of state. Therefore, it has found numerous applications in the investigations of various colloidal suspensions, including colloidal dynamics using a version of X-ray photon correlation spectroscopy in the USAXS regime.[170][171]

Much of the research focused on determining the stabilization conditions of colloidal suspensions has been devoted to monodispersed systems, whose physical description has the most clarity. Because of the introduction of a second species, the binary system adds complexity to understanding the force balance required to achieve colloidal stability. In one remarkable example,[172] Tohver *et al*. demonstrated that introducing a critical volume fraction of highly charged zirconia nanoparticles stabilizes a suspension of charge-neutral colloidal microspheres, which otherwise would flocculate due to van der Waals attractions. Competing theories emerged to explain this so-called “nanoparticle halo” phenomenon. In one case, Karanikas and Louis used a hypernetted chain integral equation closure to calculate the effective interparticle potential[173]. They found the stability is driven solely by electrostatic repulsion between nanoparticles in solution. In another case, Liu and Luijten performed Monte Carlo simulations and demonstrated a weak nanoparticle-microsphere attraction at low nanoparticle concentration leads to stabilization.[174] Yet, in neither instance is the van der Waals potential between the large spheres considered, rendering an incomplete physical description. Characterization of the fluid structure is required to provide the structural details and enable elucidation of the physical nature of the nanoparticle halo effect. However, the large size disparity between the microspheres and nanoparticles makes such measurements difficult. To meet

this challenge, we performed a series of USAXS measurements on a series of silica microsphere and zirconia nanoparticle suspensions,[175] and an example of the results is shown in Fig. 55.

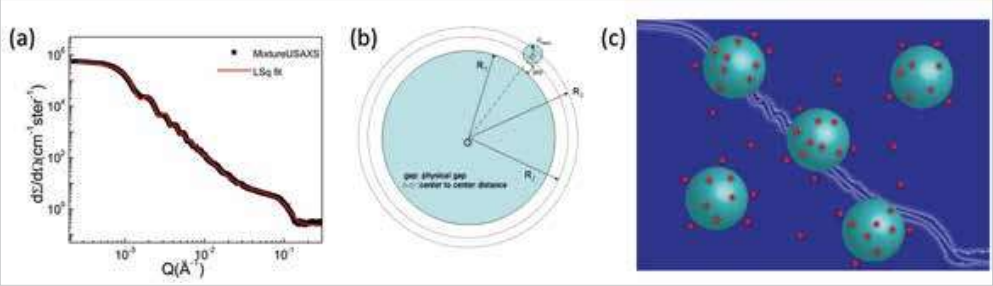

Fig. 55
(a) USAXS data of a stable suspension consisting of monodispersed, charge-neutral silica microspheres (mean radius 280 nm ± 9 nm) and highly charged zirconia nanoparticles (mean radius 2.6 nm ± 0.5 nm). (b) A core-shell model developed to analyze the scattering data. (c) An illustration of the physical picture of the dynamic nanoparticle haloing effect, where a high concentration of zirconia nanoparticles is located near, but not attached to, the microsphere surface. Adapted with permission from[175]. Copyright (2007) American Chemical Society.

Using the experimentally determined scattering form factor of the highly monodispersed uncharged microspheres and highly charged zirconia nanoparticles as input, we constructed a core-shell type scattering model (Fig. 55(b)). In this model, we allowed the physical gap and the electron density of the shell to vary to describe the mean location and the number density of the zirconia nanoparticles near the surface of the microspheres. This model described the USAXS data, shown in Fig. 55(a), very well and presented a physical picture, as illustrated in Fig. 55(c). In short, we determined the zirconia nanoparticles self-organized into a shell near the microspheres. The mean separation distance is approximately the Debye length of the solvent. Within the shell, the nanoparticle concentration is significantly higher than its bulk concentration with a lateral nanoparticle-nanoparticle separation distance ≈ of five × the nanoparticle size. These findings were later confirmed by atomic force microscope measurements,[176] providing the direct structural basis for validating theoretical predictions.

Due to space, we limit the USAXS investigation of hierarchical structure in soft materials to these two examples. However, we must reemphasize the hierarchical structures are the rule rather

than the exception in these fascinating yet complex materials that also include polymer gels, solutions, blends, micelles, vesicles, and microemulsions. USAXS provides a powerful tool for understanding the different structural levels and their roles in determining the properties and performances of these materials[177].

6.3.4 Microstructure and kinetics in hard advanced engineering materials

Andre Guinier, often considered the father of the field of small-angle scattering, first applied SAXS in 1938 to discover the formation of so-called Guinier-Preston zones in an Al-Cu alloy, a specific pre-precipitation phenomenon in alloys critical for alloy hardening.[178] Despite these early applications, soft matter research largely dominates SAXS applications in materials science. One primary reason is the limitations imposed by the limited X-ray energies from a lab-based tube or rotating anode source. In contrast to X-ray diffraction, where lab-based measurements are often conducted in the Bragg–Brentano (reflection) geometry, SAXS (GISAXS not included) requires collecting data close to the direct beam. It must be undertaken in transmission geometry. For example, the Cu source, the most used lab-based X-ray source, sits at 8.04 keV for Cu Kα radiation. For a steel sample to achieve a 5 % sample transmission, the sample thickness must be less than 15 µm. This stringent requirement creates challenges in sample preparation. It also casts questions about the measurement statistics, a key advantage of SAXS that sets SAXS measurements apart from less statistically representative electron microscope measurements. Because of these reasons, the in-house SAXS measurements for hard engineering materials, such as ceramics, alloys, and metal-ceramic composites, have lagged behind their soft materials counterparts.
The emergence of synchrotron-based SAXS during recent decades has empowered a resurgence of SAXS measurements of hard engineering materials due to its access to higher X-ray energies. Together with rapid fly-scan measurements and an additional wide-angle X-ray scattering (WAXS or XRD) detector,[150] the synchrotron

USAXS instruments enable a rare window to investigate a comprehensive structure evolution at both atomic and microstructural levels. The USAXS user community has made significant progress toward understanding a multitude of hard engineering materials, such as thermal barrier coatings,[179] cement,[180] alloys,[181][182] rocks,[183][184] and nuclear materials.[185]

In this section, we will use one example to highlight the power of comprehensive studies of the kinetic transformations of an alloy system.[186] The material, commercially available aluminum alloy 2024 (AA2024), is one of the most widely used aerospace materials due to its high yield strength, good fracture toughness, and excellent fatigue properties. This alloy is a precipitation-hardening alloy and primarily consists of Al, Cu, and Mg. Because its mechanical properties depend on the number density, location, and size of the precipitates, understanding the precipitation pathway and kinetics is essential for tailoring the material for specific applications.

We performed several insitu, isothermal experiments at different temperatures within a temperature range of 190 °C and 226 °C, typical of the precipitation heat treatment temperatures of this alloy. A solutionization heat treatment creates an identical condition for different experiments where the solute atoms are part of a supersaturated solution. Upon heating the material rapidly to the target temperature, we captured USAXS and XRD data continuously on the same sample volume as a function of time.

Fig. 56(a) shows an example of the USAXS data acquired at 226 °C. Immediately, we noticed that small, nanometer-sized clusters formed rapidly (within a few minutes) during the heating process. These clusters are similar to what Guinier identified in his aforementioned groundbreaking work on Al-Cu alloys, commonly assumed to be precursors to an equilibrium phase. As time proceeds, our data show that these clusters dissolve entirely, and the second type of large precipitates forms. TEM data of this study[186] provides conclusive evidence that the later-formed precipitate is the primary strengthening phase called the S phase. The in situ XRD

data, shown in Fig. 56(b), also corroborates TEM results regarding the formation of the S phase and the lack of long-range order of the co-clusters. Importantly, our results demonstrate the absence of S″, a controversial transient, nonequilibrium phase speculated to exist in the transformation sequence between co-clusters and the S phase.

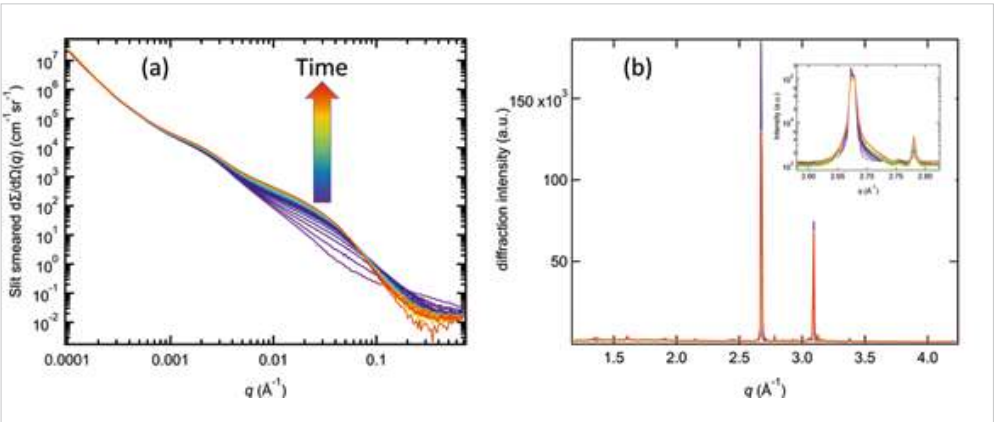

Fig. 56
(a). Time-dependent USAXS data acquired on a commercially available aluminum alloy 2024 during isothermal heat treatment at 226 °C. During this heat treatment, the GPB zones dissolve, and S phase precipitates form. (b) XRD datasets acquired simultaneously with the USAXS data, showing the development of the S phase precipitates during the isothermal heat treatment. More details can be found in [186].

Equipped with the time-dependent data, we could determine the kinetic energies required for the dissolution of the clusters and the formation of the S phase precipitates. The kinetic data demand additional attention because they form a rigorous basis to validate and benchmark predictions made by computational materials science methods, such as Computer Coupling of Phase Diagrams and Thermochemistry (CALPHAD). These computational tools, equipped with machine learning methods, have become increasingly essential to probe the large-parameter space routinely encountered in engineering materials for materials discovery and optimization. Structure- and microstructure-based kinetic datasets are the starting points for such modeling efforts. The capabilities afforded by USAXS and its accompanying SAXS and WAXS are still under-exploited and require more community awareness to unleash their full potential.

To conclude, USAXS, as a statistically significant probe, provides unique measurement capabilities for dimensional metrology. Depending on the source, optics, and accompanying instruments (SAXS and WAXS), a USAXS facility or a desktop SAXS instrument equipped with a USAXS module can cover over five orders of magnitude in sizes, from sub-Angstrom to several μm. USAXS has also evolved from a once-niche technique only available at the synchrotron X-ray facilities to a mainstream measurement tool offered by commercial SAXS equipment vendors. USAXS is also proving to be a powerful technique to enable the across-length-scale structural characterization of a wide range of materials ranging from advanced materials such as alloys and batteries to everyday encounters such as wood and chocolate. These structural data are essential to constructing the processing-structure-property relationships of advanced material, technological building blocks for a 21st-century economy. The recent development in the X-ray sources in synchrotron X-ray and desktop sources is leading to faster and better USAXS measurements and promises an even brighter future for USAXS instruments. We foresee USAXS playing a critical role in advancing materials research, development, and innovation across many industrial sectors.